Robust Real-Time Lane Delimiting Features Extraction

Radu Danescu, Sergiu Nedevschi
Technical University of Cluj Napoca
Radu.Danescu@cs.utcluj.ro, Sergiu.Nedevschi@cs.utcluj.ro

Abstract

This paper presents a robust lane marking detection algorithm suited for a large variety of traffic scenarios, under various lighting conditions. The algorithm detects dark-light-dark transitions using an improved method for horizontal gradient computation, which accounts for the expected marking width and for the perspective effect by means of a variable size filter. The computation of the variable filter-based gradient is optimized for real-time operation by reusing the intermediate results of the neighboring pixels. Stereovision is used for final filtering of the results, by selecting only the marking-like features located on the road surface.

1. Introduction

Lane detection, a problem that has been extensively researched for many years, is a crucial component of the driving assistance systems and of the autonomous robot navigation systems. The research in the lane detection field continues, because so far no solution is both complete, fast, easy to set up and error free. Most researchers have decomposed the problem of lane finding in two sub-problems: lane delimiter feature extraction and 3D or 2D lane model matching. The weight of each of the sub-problems may differ: a simple feature extraction algorithm can operate well with a complex, elaborate model matching technique, or vice versa. Ideally, one must try to extract the best of both sides, but compromise must be often made for the sake of real-time operation.

Lane delimiter feature extraction algorithms traditionally use the grayscale monocular image as input data. The features that are found can be simple gradient maxima [1], edges extracted by Canny-compliant edge detectors [20], [2], edge-like elements that have a constrained orientation obtained through frequency domain analysis [9], eigenvalues of the moment matrices [16] or steerable filters [12]. The aforementioned features are mostly edges, which do not take into account the particularities of the lane markings: light strips of expected width on a darker background. This particularity is exploited in [6], where it is detected as a pair of gradient values of similar magnitude and opposing signs (the dark-light-dark, DLD, transition) and in [10] where, after a segmentation, the lighter image regions that have an expected width (conditioned by the perspective effect) are taken into account and in [7] through a segmentation step followed by a complex classification of the lighter segments using their geometrical properties and a decision tree framework. An elaborate lane marking detection method, presented in [3], uses the Inverse Perspective Mapping (IPM) to compensate for the variable lane marking width in the image space, and then filters the resulted image with a marking width-conscious filter, followed by adaptive thresholding.

Other lane delimiting feature extraction methods use color images, on which they perform segmentation either by using the original RGB color space [5], the HSI color space [17] or combinations of color and texture [4]. Almost all color –based techniques are, to a certain degree, segmentation algorithms.

Stereovision is another tool for lane delimiter feature extraction. The 3D information associated to image features (which can be edges, points, blobs, etc) helps select the ones located on the road, minimizing the effect of obstacle features on the lane detection process. The reasoning for road feature selection can be performed either on the 3D coordinates, as in [14], or on the image coordinates augmented by the stereo disparity [19].

Lane delimiting information can be extracted also by the use of active sensors, such as RADAR and LASER. The classical use of such sensors generates a polar range map, which is limited from the lane detection point of view, but can extract the general limits of the road itself (guardrails, pillars, etc). A lane detection method based solely on laserscanner is presented in [8]. Radar is used to help an image-based lane detection process in [11]; in [18] laser is used for near curb detection, while providing a starting search zone for the forward-looking image-based algorithms. Recent laser and radar technologies allow the development of active sensors that provide range and reflectivity images instead of a simple distance "slice", and these images can be processed like normal images [13] or they can be combined with color images to help the road segmentation [15].

The method described in this paper is centered on the classical DLD transition paradigm, but brings significant improvements in the way these transitions are detected. The gradient is computed using a variable size filter, targeted for the desired marking width and adjusted with the image's perspective effect. Real time computation of this gradient is achieved through "software pipelining", by reusing the intermediate values of the neighboring pixels. Another improvement is the use of stereovision to filter out the features that are not located in the road plane. The resulted algorithm is a robust and real-time lane marking extractor suitable for all marked roads (urban and non-urban).

2. Principle

The lane marking is usually white, or anyway it has a lighter color than the rest of the road surface. If one scans over the lane marking horizontally, the perceived intensity will vary in a specific Dark-Light-Dark (DLD) pattern. This property is not influenced by shadows, unless the shadow ends in the middle of the road marking, a highly unlikely event. In [7] this DLD transition is detected as a pair of gradient values of similar magnitude and opposing sign.

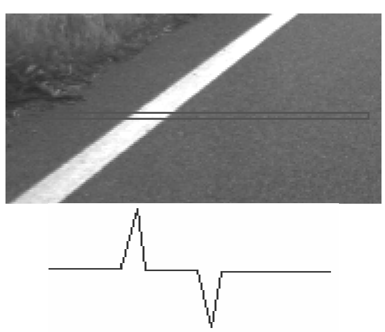

Figure 1. The horizontal gradient for a lane marking. Dark-light-dark transition is encoded in the gradient

The problem is that the perspective effect affects the perceived level of detail of the road surface. The closest visible road part presents a richness of texture, even if the road is asphalt only, while for the farthest part even the markings are barely visible. A gradient computed with a constant size mask, such as the one that's used for a full-image, all-purpose edge detection, assumes that at any point in the image the level of detail is the same. A small differentiation kernel (i.e., the Sobel filter), will extract the edges corresponding to the far markings, but it will also extract false edges, corresponding to the noisy road texture, for the near part of the road. This is not, however, the most dangerous side effect of using a fixed size kernel. The transition between light and dark (as it is the case for lane markings) will not occur in the same number of intermediary values for a near marker and for a far marker, and therefore the gradient values may be smaller for the near markings (transition is smoother). If the resulted gradient is too low, the edge may be missed completely.

A general-purpose filter is suitable for obstacle detection, as their distance is unknown and there is no way of knowing the level of detail a priori. The lane case is different: the road is mostly flat, we know the position of the camera with respect to the road, and we know a minimum acceptable width of the lane marking. This way, we can predict the minimum width of the marking for each position in the image, using the perspective effect.

3. Algorithm description

3.1. Computing the horizontal gradient using an adaptive size mask

The way in which we establish the width of the marking in the image is very simple: by projecting a point of coordinates (*X=0, Y=0, Z=infinity*) in the image plane, we establish the vanishing line. This is the topmost image line containing road information. On this line, the size of the road marking is zero. By projection of two points, ($-w/2$, 0, Z_L) and ($w/2$, 0, Z_L), Z_L being the minimum distance where the road gets visible in the image and w being the minimum road marking width, we obtain the image width of the lane marking for a lower image line. The width of the differentiation filter for the other image lines will be computed by linear interpolation. The process is illustrated in figure 2.

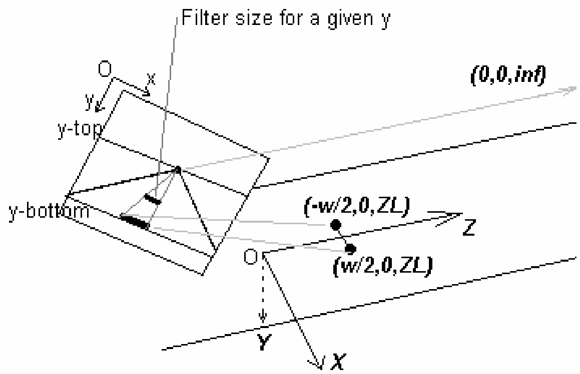

Figure 2. Computing the width of the differentiation filter

The smallest filter will be [-1 0 1], at the horizon line, and the general filter will have the form [-1 -1 … -1 0 1 1 .. 1]. One may object that the method of evaluation of the kernel's width does not account for the possible changes of pitch angle, or of vertical curvature. The answer is that this is just estimation, and does not have to be exact. It just tries to account for the variable level of detail. A small variation of pitch or vertical curvature does not change things dramatically, especially not for the close road regions, which are most affected by the variable width filtering.

The value of the horizontal gradient of a point of coordinates (x, y) is given by equation 1.

$$G_N(x,y) = \frac{\sum_{i=x+1}^{x+D} I(i,y) - \sum_{i=x-1}^{x-D} I(i,y)}{2D} \qquad (1)$$
$$D = KernelSize(y)$$

Applying the above formula directly is computationally expensive, as D's value may even go beyond 20, for the lowest image lines. However, we can observer that the gradient of a point differs very little from the gradient of its previous neighbor. For that, we have to defer the division by 2D to the end of the computation. Let's denote the un-normalized gradient by G_U:

$$G_U(x,y) = \sum_{i=x+1}^{x+D} I(i,y) - \sum_{i=x-1}^{x-D} I(i,y) \qquad (2)$$

Then we have a recurrent equation:

$$G_U(x,y) = G_U(x-1,y) + I(x+D,y) - I(x,y) + I(x-D-1,y) - I(x-1,y) \qquad (3)$$

This means a fixed computation time for each step. Off course, this gain is felt for D>=3, otherwise it is faster simply to apply equation (1). Normalization takes place at the end of each line.

$$G_N(x,y) = \frac{G_U(x,y)}{2D} \qquad (4)$$

The final step is to average each gradient value with the values of its top and bottom neighbors, for increased stability. This is equivalent to having a 3x(2D+1) size filter for horizontal gradient computation through convolution.

The result of applying the adaptive differentiation filter is presented in figure 3. The zero value of the gradient is represented as image intensity 128, so that both negative and positive values can be shown.

Fig. 3. Original grayscale image (top) and the result of applying the adaptive horizontal gradient filter (bottom)

3.2. Non maximum / minimum suppression

We have to identify the lane marking edges, and therefore non-extreme suppression is performed on the image resulted from the adaptive horizontal gradient filtering. As a wider kernel sometimes means a slower variation of the gradient as the distance from the edge increases, we have made a small modification to the non-maximum suppression technique. The classical non-maximum suppression conditions are something like:

If I(x,y)<I(x-1, y) **or** I(x,y)<I(x+1,y) **then** I_{dest} (x,y) = 0

Our non-maximum suppression conditions are a little different:

If I(x,y)<I(x-1, y) or I(x,y)<I(x+1,y) **then** I_{dest} (x,y) = 0
Else
    If I(x,y)=I(x-1, y) **and** I(x,y)<I(x-2,y) **then** I(x,y)=0
Else
    If I(x,y)=I(x+1, y) **and** I(x,y)<I(x+2,y) **then** I(x,y)=0

Basically, we include the neighbors' neighbor into the comparison. The result of this non-extreme suppression is shown in figure 4.

Figure 4. Results of non-maximum/minimum suppression

3.3. Finding DLD pairs

For each of the resulted maxima, a search for the corresponding minimum is performed. The interval of the search is given by the minimum and maximum possible lane marking widths for the specific image line.

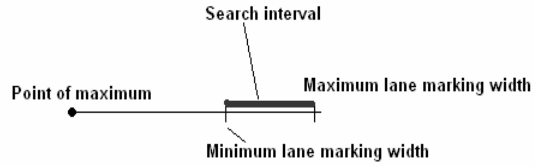

Figure 5. The interval for pair search

The pair gradients must be similar in magnitude and opposed in sign. The similarity is computed by the following formula:

$$S(M1, M2) = \frac{abs(M1 - M2)}{\max(M1, M2)} \quad (5)$$

A pair is found if the similarity measure is lower than a threshold *T*. This threshold can have two values: T_{low} = 0.3, and T_{high}=0.5. The selection between one of the two possible threshold values depends on the average brightness of the points between the point of maximum and its possible pair. If this brightness is higher than 200, the selected threshold is T_{high}, otherwise the selected threshold is T_{low}. This follows a simple line of thought: if the surface between the two possible marker edges is bright, we are more certain that this is in fact a marker, and therefore we can relax the conditions of gradient similarity. Otherwise, we cannot rely on brightness to give us a cue about the possible marker existence, and we need to tighten the conditions so that we can avoid the false positives. The value 200 was chosen rather arbitrarily, and a possible automatic selection, based on the average image intensity may yield better results.

The points of very low gradient magnitude are eliminated in this step. The result of the dark-light-dark pairing process is shown in figure 6.

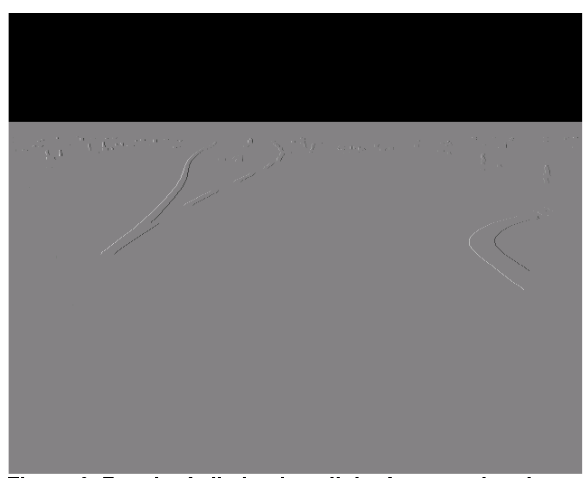

Figure 6. Result of eliminating all the features that do not obey a dark-light-dark pattern

3.4. Selecting only the road features, using the 3D information

All the processing so far has been 2D processing, aided by a little information about perspective. Stereovision provides the 3D information for the points that remain after step 3, and we can therefore eliminate the features that don't belong to the road surface. A method for extracting the parameters of the vertical profile of the road surface (pitch and vertical curvature) was described in [14].

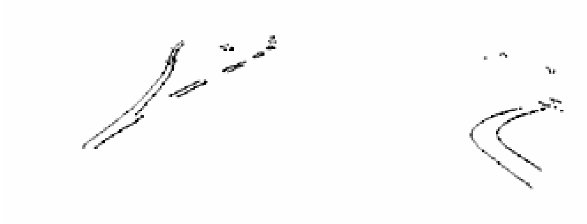

Figure 7. The final lane marker detection result

4. Results

The feature extraction algorithm is part of a stereovision-based lane and obstacle detection system for that can operate in real-time on highways and in the urban scenarios. The lane detection algorithm can work on simple road edges, in the absence of lane marking classification, but lane marking features take priority, when present. For this reason, the lane marking detector must focus on robustness, not on completeness (it is better to have less detected markings, as they are also edges, than to have false positives of high priority).

The algorithm was tested in a large variety of scenarios, from highway to urban and rural, in multiple lighting conditions and with different camera setups (different focal lengths, different imaging sensors) and it has proven to be robust and scenario independent. The markings were detected almost all the time, provided they looked like markings (not too dirty or too thin), and the only false positives are caused by structures that cannot be differentiated from lane markings without the help of a larger context.

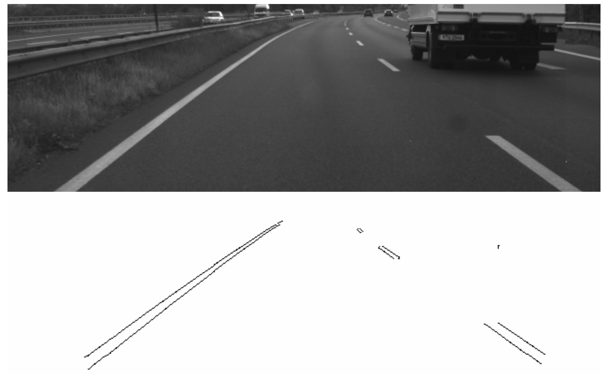

Figure 8. Detected features in a classical highway scenario – clear markings

Figure 9. Detected features in urban scenario – clear markings

Figure 10. Detected features in rural scenario – saturated markings, low contrast, plenty of noise features on the ground

Figure 11. Detected features in urban scenario – worn markings, very low contrast

5. Conclusion

The use of a variable size filter that accounts for the variation of the lane marking width with the perspective effect proved to be a powerful tool for dealing with the variable level of detail and with near range noise texture, without the use of costly and damaging low past filters. The implementation of this filter came without any significant computation cost increase, due to the ingenious use of the partial results of the pixel neighbors. In this way we have increased the robustness and performance of a classical lane marking detection technique, the dark-light-dark transition detector, and we have obtained an excellent all-purpose lane delimiting feature extractor.

6. References

[1] R. Aufrere, R. Chapuis, F. Chausse, ”A model-driven approach for real-time road recognition”, *Machine Vision and Applications, Springer-Verlag 2001*

[2] R. Aufrere, V. Marion, J. Laneurit, C. Lewandowski, J. Morillon, R. Chapuis, “Road sides recognition in non-structured environments by vision”, *IEEE-IV 2004*

[3] M. Bertozzi, A. Broggi, “GOLD: A Parallel Real-Time Stereo Vision System for Generic Obstacle and Lane Detection”, *IEEE Transactions on Image Processing, Vol. 7, January, 1998*

[4] N. W. Campbell, B. T. Thomas, “Segmentation of Natural Images using Self-Organizing Feature Maps”, *British Machine Vision Conference (BMVC) , 1996*

[5] J.D. Crisman, C. E. Thorpe, “UNSCARF, A Color Vision System for the Detection of Unstructured Roads”

[6] J. Goldbeck, B. Huertgen, “Lane Detection and Tracking by Video Sensors”, *In Proc. IEEE International Conference on Intelligent Transportation Systems, October 5-8, 1999, Tokyo Japan, pp. 74–79.*

[7] J.P. Gonzalez, U. Ozguner, “Lane Detection Using Histogram-Based Segmentation and Decision Trees”, *in Proc. IEEE-ITS, 2000, pp. 346–351*

[8] A. Kirchner, Th. Heinrich, “Model based detection of road boundaries with a laser scanner”, *IEEE-IV 1998*

[9] C. Kreucher, S. Lanksmanan, “LANA: A Lane Extraction Algorithm that Uses Frequency Domain Features”, *IEEE Transactions on Robotics and Automation, 1999*

[10] R. Labayrade, S. S. Ieng, D. Aubert, “A Reliable Road Lane Detector Approach Combining Two Vision-Based Algorithms”, *IEEE-ITSC 2004*

[11] B. Ma, S. Lankshmanan, A. Hero, “Road and Lane Edge Detection with Multisensor Fusion Methods”, *IEEE, 1999*

[12] J. C. McCall, M. M. Trivedi, “An Integrated, Robust Approach to Lane Marking Detection and Lane Tracking”, *IEEE-IV 2004*

[13] U. Meis, R. Schneider, “Radar image acquisition and interpretation for automotive applications”, *IEEE-IV 2003*

[14] S. Nedevschi, R..Schmidt, T. Graf, R. Danescu, D. Frentiu, T. Marita, F. Oniga, C. Pocol, “3D Lane Detection System Based on Stereovision”, *IEEE Intelligent Transportation Systems Conference (ITSC), 2004, Washington, USA*

[15] C. Rasmussen, “Combining Laser Range, Color, and Texture Cues for Autonomous Road Following”, *IEEE Conference on Robotics and Automation, 2002*

[16] R. Risack, P. Klausmann, W. Kruger, W. Enkelmann, “Robust lane recognition embedded in a real-time driver assistance system”, *IEEE-IV 1998*

[17] M. A. Sotelo, F. J. Rodriguez, L. Magdalena, L. M. Bergasa, L. Buquete, “A Color Vision-Based Lane”, *Autonomous Robots, Kluwer Academic Publishers, 2004*

[18] C. Thorpe, R. Aufrere, J.D. Carlson, D. Duggins, T.W. Fong, J. Gowdy, J. Kozar, R. MacLachlan, C. McCabe, C. Mertz, A. Suppe, C. Wang, and T. Yata, “Safe Robot Driving”, *Proceedings of the International Conference on Machine Automation (ICMA 2002), September, 2002.*

[19] J. Weber, M. Atkin, “Further Results on the Use of Binocular Vision for Highway Driving”, SPIE 1996

[20] B. Yu, A. K. Jain, “Lane Boundary Detection Using A Multiresolution Hough Transform”, *IEEE International Conference on Image Processing (ICIP), 1997*